J Therm Anal Calorim (2011) 105:535–544
DOI 10.1007/s10973-010-1224-8

Thermochemistry of triboactivated natural and NH_4-exchanged clinoptilolite mixed with Tunisian apatite

V. Petkova · E. Serafimova · N. Petrova ·
Y. Pelovski

ESTAC2010 Conference Special Issue

Abstract Mechanical tribo- and thermo-chemical methods applied for remodeling phosphate raw materials manifest a number of advantages over the conventional technologies. They are related to the reduction of soil contamination and minimization of the released gas emissions in the environment and generate solid wastes. In this work, natural and NH_4-exchanged clinoptilolite are used for increasing the transition of P_2O_5 into assimilated by plants form during tribochemical activation (TCA). Better nutrients assimilation as well as green production could be achieved by applying such a treatment based on the ion-exchange reactions taking place in the soil. The occurring upon TCA structural changes and phase transformations of the used Tunisian phosphorite, natural and NH_4-exchanged clinoptilolite as well as their mixtures are investigated by means of X-ray powder diffraction, IR spectroscopy, and thermal analysis. The thermal method gives evidence for solid phase reactions and increased reactivity as a result of the tribochemical treatment. This treatment leads also to minimization of the size of crystallites, amorfization of the samples, and increasing amount of hydroxyl and carbonate ions in the apatite structure. Treated samples are highly soluble. In addition, conditions for almost complete solubility of P_2O_5 were found. This study shows that some of the produced compositions are suitable for fertilizers or soil conditioners.

Keywords Apatite · Clinoptilolite · Tribochemical activation · Thermal decomposition

Abbreviations

Ap ($Ca_5(PO_4)_3F$)	Tunisian apatite
Nat-Cpt	Natural clinoptiolite
NH_4-Cpt	NH_4-exchanged clinoptiolite
TCA	Tribochemical activation
TCM	Tribochemical mixing
C-F-Ap ($Ca_{10}(PO_4)_5CO_3$)	Carbonate fluorine apatite
C-OH-F-Ap ($Ca_{10}(PO_4)_5CO_3(OH)F$)	Carbonate hydroxyl fluorine apatite.

Introduction

The depletion of natural resources, climate changes, and ecological balance disturbance as a result of human industrial activities are among the main problems of the day. These problems put questions for the comprehensive utilization of the mineral raw materials, the product quality, and the environmental protection.

Natural apatite is the main raw material for production of mineral fertilizers. The application of traditional technologies for acidic receipt creates environmental problems associated with environmental contamination with solid phases and gaseous wastes. This is the reason to seek new methods and technologies for obtaining useful products

---

V. Petkova (✉) · N. Petrova
Institute of Mineralogy and Crystallography, Bulgarian Academy of Sciences, Acad. G. Bonchev Str. Bl. 107, 1113 Sofia, Bulgaria
e-mail: vilmapetkova@gmail.com

E. Serafimova · Y. Pelovski
University of Chemical Technology and Metallurgy, 8 Kl. Ohridski Blvd., 1756 Sofia, Bulgaria

based on a low-quality materials such one as the tribochemical treatment [1, 2].

Natural clinoptilolite is a mineral of volcanic activity origin forming large industrial deposits. Added in the soil, this zeolite improves the soil structure and act favorably on the soil fertility due to its high ion-exchange capacity. Clinoptilolite has been shown to slow nitrification by 11%, to reduce nitrate leaching by 30%, to increase ammonium and potassium retention, to reduce ammonia volatilization, and slowly release NH_4^+, K^+, and other plant nutrients [3].

Tribochemical activation (TCA) of natural phosphates and natural zeolites is an unusual decision to address environmental and resource problems aiming at higher level of transition of non-assimilated P_2O_5 into assimilated by plants forms using synergic useful properties of both materials [4–6]. In this study, two samples of clinoptilolite—natural and NH_4-exchanged were mixed in various ratios with natural phosphorite and treated in two modes: tribochemical mixing (TCM) and activation.

Application of thermal methods together with infrared spectroscopy and X-ray diffraction analysis allows to study the structural and phase transformations in the apatite–clinoptilolite system with a focus on the changes that occur during TCA. The results obtained will be used to establish the optimal conditions of mixing and activation, the thermal stability of selected compositions, and the influence of impurities in used raw materials on the effects of their processing.

Methods

The TCA was carried out in a planetary mill Pulverisette-5, Fritsch Co (Germany) at a rotating speed of 280 min^{-1}, activation time 240 min, type of milling bodies—agate, diameter of the milling bodies 5 mm, sample mass 10 g. TCM was performed in an agate mortar for 10 min.

A standardized method for determination of $P_2O_5^{ass}$ was used following:

- Bulgarian National Standard 14131-88, according to which $P_2O_5^{ass}$ was determined by direct extraction in solution of ammonium citrate with pH = 7 or by 2% citric acid;
- Instruction of EEO 77/535 p. 3.1.4 “Extraction of phosphorus soluble in neutral ammonium citrate” as the dragging out of $P_2O_5^{ass}$ was performed by direct extraction.

Thermogravimetric and differential thermal analyses (TG–DTG–DTA) were performed on a Stanton Redcroft thermal analyzer STA 780 (England) in the temperature range 20–1000 °C, with a heating rate of 10 $°C.min^{-1}$, sample mass of 10.0 ± 0.2 mg. Zirconium melting pots of $d = 4.5$ mm were used and the purging gas was synthetic (100% purity) dry air and flow-rate 50 mL min^{-1}.

The powder X-ray diffraction (XRD) measurements of the samples were performed on D2 Phaser Bruker AXS, using a Ni-filtered Cu K_α radiation ($\lambda = 0.15418$ nm). A step-scan technique was applied with a step size of 0.05° 2θ and 3 s per step in the range 8°–70° 2θ.

Phase identification was performed using the index file PDF (Powder Diffraction File, ICDD, 2001).

The Fourier transform infrared (FTIR) spectra were taken on a Bruker Tensor 37 spectrometer, using KBr pellet technique. A resolution of 2 cm^{-1} was used collecting 120 scans for each sample.

Materials

Natural clinoptilolte (Nat-Cpt) from Beli Plast deposit, Bulgaria and natural apatite (Ap) from a Tunisian deposit were used for the purpose of this study.

The chemical composition of apatite is presented in Table 1.

The origin of Tunisian phosphate is related to phosphate minerals obtained by precipitation from sea water. Phosphate mineral ores are complex systems in terms of mineral composition and to the apatite structure, which exhibits a tendency towards cationic and anionic isomorphism. Tunisian phosphorite [1] refers to the group of “core” apatite with a ratio (Ca/P) = 1.70–1.77. These apatites are formed in calcium phosphate-systems with pH > 7 and are characterized by increased defectiveness and isomorphic anionic substitutions (mainly by carbonate ions). Tunisian phosphorite is defined as carbonate apatite fluorine (C-F-Ap). Mineralogically the Ap consists mainly of francolite (about 94%). The main impurity minerals are calcite, dolomite, feldspar, and quartz.

The clinoptilolite tuff contains about 80 wt% clinoptilolite and admixtures of montmorilonite, biotite, seladonite, low-crystobalite, quartz, and feldspars. The chemical composition of isolated clinoptilolite (wt%) is: SiO_2—66.15; Al_2O_3—11.31; Fe_2O_3—0.67; MgO—0.46; CaO—4.20; Na_2O—0.34; K_2O—3.13; H_2O—13.92.

Table 1 Chemical composition of Tunisian phosphorite concentrate (wt%)

$P_2O_5^{total}$	CaO	SO_x	SiO_2	CO_2	Cl_2	R_2O_3	Na_2O	K_2O	MgO	F_2
29.58	48.40	3.58	1.88	6.48	0.017	1.07	1.38	0.07	0.67	2.74

The clinoptilolite tuff sample was treated with 1 M solution of NH_4NO_3 by shaking for 3 days at 60 °C changing the solution each day and finally washed and dried at room temperature. Since the ammonia ions occupy all cationic positions in the clinoptilolite channels by this treating a mono-ionic form was prepared [7]. It was shown that the total cation exchange capacity (CEC) with respect to Al content for Beli Plast clinoptililite is 2.2 meq g^{-1} as the degree of ion exchange with NH_4^+ is higher than 98% [8].

Three mixtures prepared of natural or NH_4-exchanged clinoptilolite (NH_4-Cpt) and Tunisian apatite with the following mass ratios, 80:20, 50:50, and 20:80 were treated by TCA and TCM. Samples of Ap, Nat-Cpt, and NH_4-Cpt were individually treated, as well.

Results and discussion

Characteristics of the initial samples (Nat-Cpt, NH_4-Cpt, and Ap)

The most informative method regarding isomorphic substitutions in the Ap structure and cation exchange in the Cpt structure is the IR spectroscopy. IR spectra of Nat-Cpt, NH_4-Cpt, and Ap are presented in Fig. 1.

The presence of NH_4-ion stabilizes the zeolite structure. An asymmetric (ν_4) bending mode of the ammonium group (1400–1450 cm^{-1}) is clearly expressed in the IR-spectrum of NH_4-Cpt in Fig. 1.

The introduction of carbonate ion in the apatite structure is evidenced by the presence of bending (ν_2) (866 cm^{-1}) and vibration stretching mode (ν_3) in the range 1430–1460 cm^{-1}. These bands define the type of C-F-Ap as B-type [1, 9]. Within the vibrational bands (ν_1) of the hydroxyl anion—3400–3600 cm^{-1}, an insertion of a low intensity peak is established, which moves the center of the peak at 3430 cm^{-1}. This fact is related to the presence of a structurally bonded hydroxyl ion in the apatite. The peak position at 3536 cm^{-1} shows partial substitution of F^- with OH^- and fluorine-formation of hydrogen bonds (O–H···F) in the apatite structure [10, 11]. This means that in addition to the isomorphic substitution of phosphate ion by carbonate one, an implementation of hydroxyl ion in the position of fluorine occurs. From these data, the used Ap sample in this study is identified as carbonate hydroxyl fluorine apatite.

Chemical analysis

The suitability of phosphorus fertilizers for plant's assimilation is determined by the solubility of their main useful component—P_2O_5. Based on their solubility, phosphate fertilizers are referred to as water-soluble and/or assimilable.

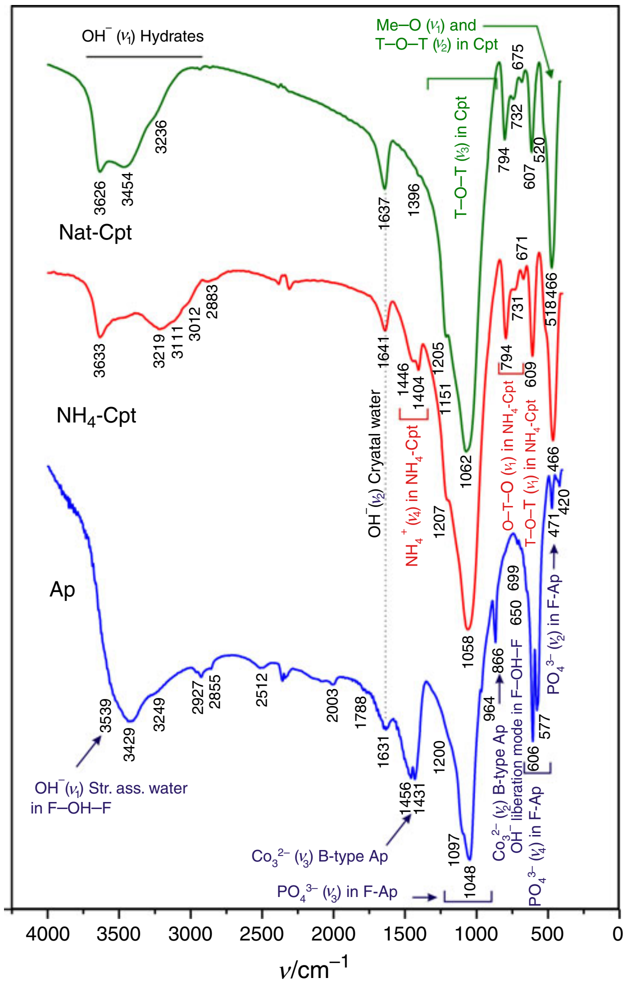

Fig. 1 IR spectra of Nat-Cpt, NH_4-Cpt, and Ap

The assimilated fertilizers are hardly soluble in water, but their active component (expressed as $P_2O_5^{ass}$) can be absorbed by plants when dissolved in solvents like soil solution. Estimation for appurtenance of fertilizers to this group will be based on their solubility in the so-called conventional solvents—solution of ammonium citrate (citratum soluble fertilizers) or 2% solution of citric acid (citric soluble fertilizers). The choice of both reagents is based on their similarity with the soil solution. In recent years, assimilated fertilizers have priority because of their slower solubility as compared with that one of water-soluble fertilizers.

Results of chemical analysis concerning the solubility of mixtures of Nat-Cpt/Ap and NH_4-Cpt/Ap by 2% citric acid are presented in Table 2.

The presented results on Nat-Cpt/Ap or NH_4-Cpt/Ap mixtures of various ratios indicate high degree of transition of P_2O_5 into assimilated by plants form in both cases of treating. The explanation of these results varies for each particular case of mixing and treating:

Table 2 Solubility of mixtures of Nat-Cpt/Ap and NH_4-Cpt/Ap by 2% citric acid

Sample/mixture	Content of $P_2O_5^{ass}/P_2O_5^{total}$/% for Nat-Cpt/Ap		Content of $P_2O_5^{ass}/P_2O_5^{total}$/% for NH_4-Cpt/Ap	
	TCM	TCA	TCM	TCA
0 (100% Ap)	28.90	64.71	28.90	64.71
20:80	70.69	87.58	70.10	85.22
50:50	71.07	89.48	85.43	93.91
80:20	95.02	88.24	99.20	86.96

- The TCM tolerates ion-exchange reactions in the systems:

$$\text{Apatite rock} + (\text{K, Na})\text{-Nat-Cpt} \overset{\text{Soil solution}}{\leftrightarrow} \text{Ca-Cpt} + (\text{K}^+, \text{Na}^+)_{\text{solution}} + (\text{H}_2\text{PO}_4^-)_{\text{solution}} \quad (1)$$

$$\text{Apatite rock} + \text{NH}_4\text{-Cpt} \overset{\text{Soil solution}}{\leftrightarrow} \text{Ca-Cpt} + (\text{NH}_4^+)_{\text{solution}} + (\text{H}_2\text{PO}_4^-)_{\text{solution}} \quad (2)$$

The effect of ion-exchange reaction is manifested in great manner when NH_4-Cpt dominates (Table 2). NH_4-zeolite acts as a sink for Ca^{2+} during exchange, thereby releasing NH_4^+ and lowering the activity of Ca^{2+} in solution. With a lower Ca^{2+} activity in solution, more apatite will dissolve [12]. The combination of dissolution and ion-exchange reaction is more advantageous than applying each of the methods separately because both reactions drive each other [3].

- The TCA leads to decrease of the zeolite ion-exchange ability. At the same time the activation increases the apatite reaction ability and solubility.

Chemical analyses give ground to suggest that some structural changes have occurred during the TCA in both components. This needs further evidences by other methods.

Thermal analysis

Thermal studies of Nat-Cpt, NH_4-Cpt, and Ap, and their mixtures upon TCM and TCA are presented in Figs. 2, 3, 4, 5, and 6 and in Tables 3 and 4.

Thermal behavior of Nat-Cpt, NH_4-Cpt, and Ap, and their mixtures upon TCM

Thermal behavior of clinoptilolite (Fig. 2; Table 3) is determined mainly by the so-called "zeolitic water" which releases up to 600 °C and strongly depends on the type of cations in the channels of the zeolite structure [13, 14]. TG–DTG curves of both Nat-Cpt and NH_4-Cpt show identical decomposition process. Basically the process develops up to 600 °C and is accompanied by 12.5–13.8% mass loss related to the gradual dehydration of zeolitic water. Zeolite structure collapse occurs with increasing temperature verified by XRD analysis (Table 5).

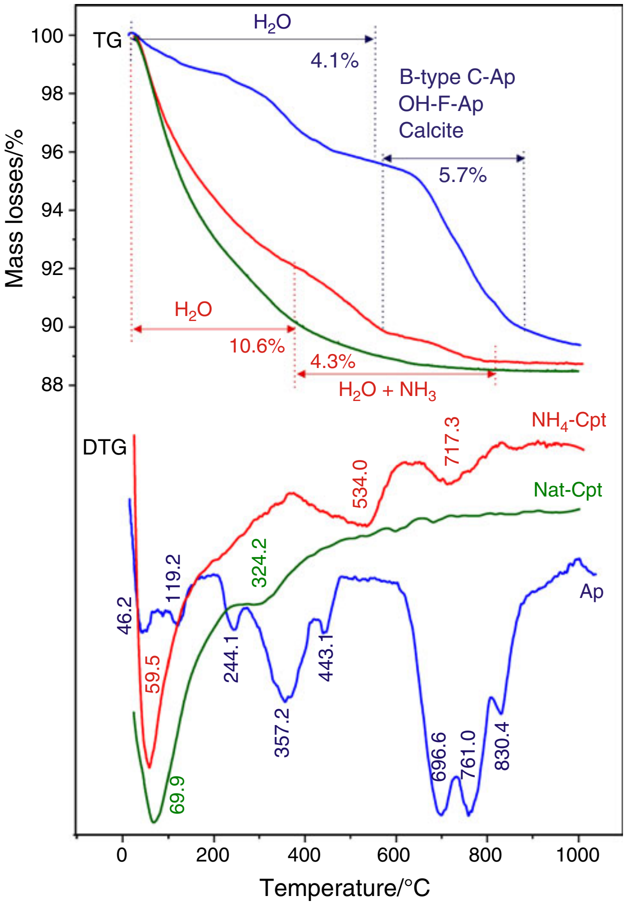

Fig. 2 TG–DTG of initial Ap, Nat-Cpt, and NH_4-Cpt

In the case of NH_4-Cpt the main stage of dehydration is performed up to 400 °C (about 10% mass loss). Deamonization runs in two stages (534.0 and 717.3 °C, Fig. 2), which is explained by the different type of ammonium bonding (ionic and hydrogen, [7]) in the structure of NH_4-Cpt. The exothermal processes occurring at 568.4 and 826.0 °C (Table 3) can be ascribed to the oxidation of the released ammonia with the air into nitrogen oxides [15].

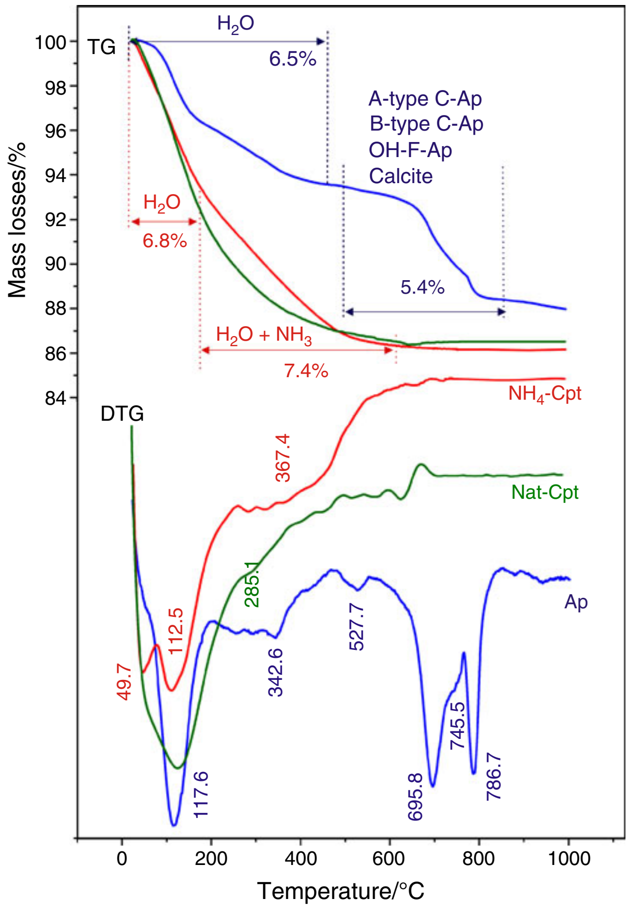

Fig. 3 TG–DTG of Nat-Cpt, NH_4-Cpt, and Ap upon TCA

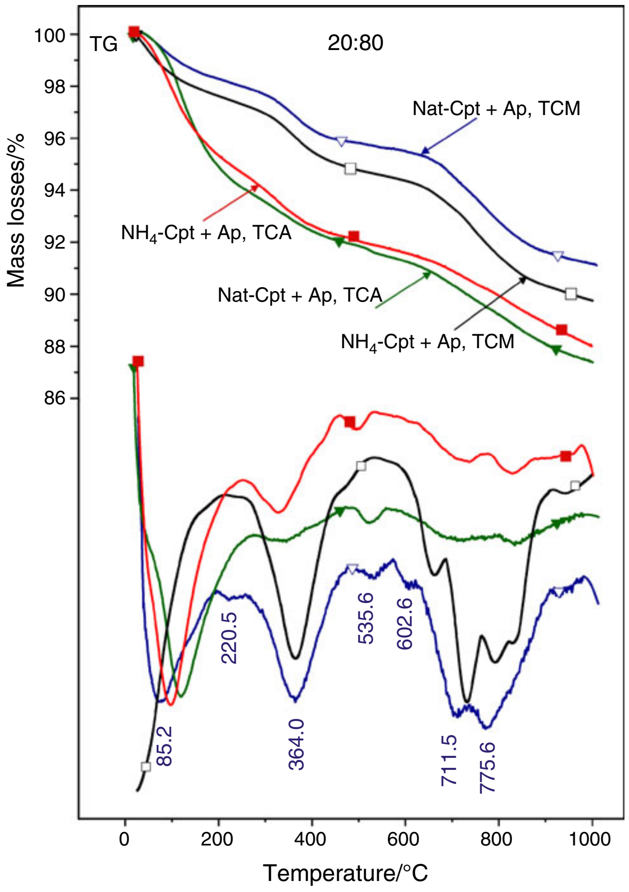

Fig. 4 TG–DTG curves of decomposition of mixtures of Nat-Cpt/Ap and NH_4-Cpt/Ap in mass ratio 20:80

The stages of dehydration and deamonization of clinoptilolite samples are finished by strong amorphization of the solid phase. XRD analysis data after heating at 1000 °C are presented in Table 5.

Tunisian phosphorite is regarded as a heat-resistant mineral, which partially decomposes at temperatures above 1000 °C. Lowering the temperature of decomposition is facilitated by cationic or anionic isomorphism and structural defects [17–21]. In the process of thermal treatment of nonactivated Tunisian phosphorite up to 1000 °C, a total mass loss of 10.8% is registered (Fig. 2) attributed to the dehydration of free, crystallization, and structurally related water, decarbonization of $CO_2{}^{3-}$ in both the structure of phosphate and carbonate impurities. The physic sorption and the associated water of crystallization are released in a wide temperature range (up to 600 °C) while both structural water and CO_2 are released after 660 °C. The endothermic effect recorded in the temperature region of 670 °C is associated with the decomposition of CO_2 localized in the tetrahedral positions of the phosphate ion in the apatite structure (Fig. 2). The main reaction is the formation of $Ca_3(PO_4)_2$ [1], which is also confirmed by the phase analysis of the solid residue after heating up to 1000 °C (Table 5):

$$Ca_{10}(PO_4)_6F_2 = 3Ca_3(PO_4)_2 + CaF_2 \quad (3)$$

Decarbonization of carbonate impurities (calcite and dolomite) occurs in the next temperature range 730–810 °C in which approximately 2% mass loss are registered. Thermal effects in the latter temperature range ($T_{\mathrm{infl}} = 830$ °C) is probably explained by the rupture of F–OH–F bonds in the apatite structure, localized on the hexagonal axis, which can be represented by the reaction (4):

$$Ca_{10}(PO_4)_6(OH)F = 2Ca_3(PO_4)_2 + Ca_4O(PO_4)_2 + HF \quad (4)$$

Only when hydroxyl ion presents in the apatite structure, it is possible to obtain $Ca_4O(PO_4)_2$ [22].

The infrared spectroscopy data which show structural-OH-related positions in the fluorine ion (Fig. 1) are another evidence for reaction (4) in addition to the reported mass losses.

Thermal decomposition of mixtures of Nat-Cpt/Ap and NH_4-Cpt/Ap at mass ratios of 20:80, 50:50 and 80:20

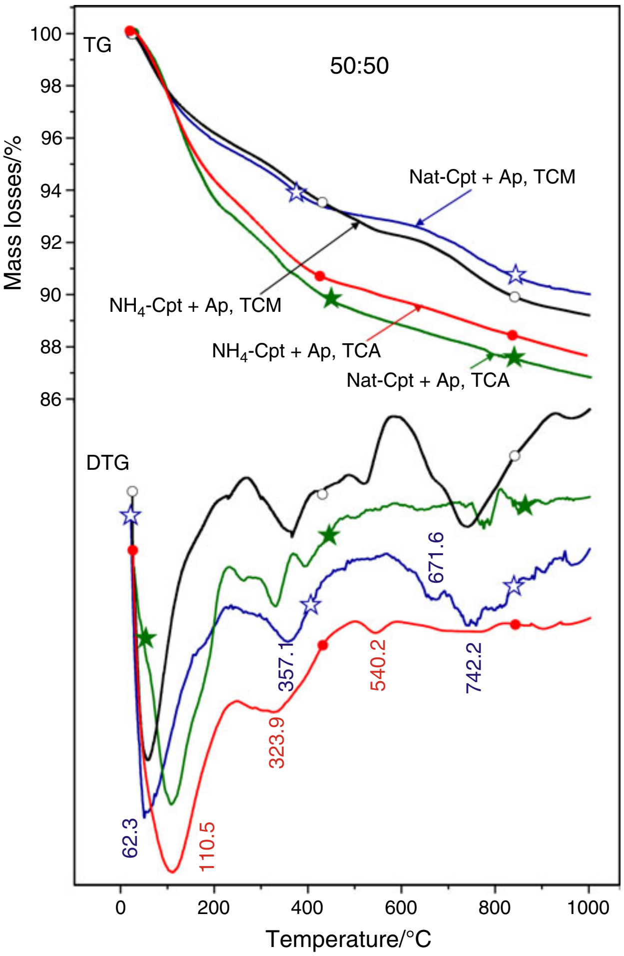

Fig. 5 TG–DTG curves of decomposition of mixtures of Nat-Cpt/Ap and NH$_4$-Cpt/Ap in mass ratio 50:50

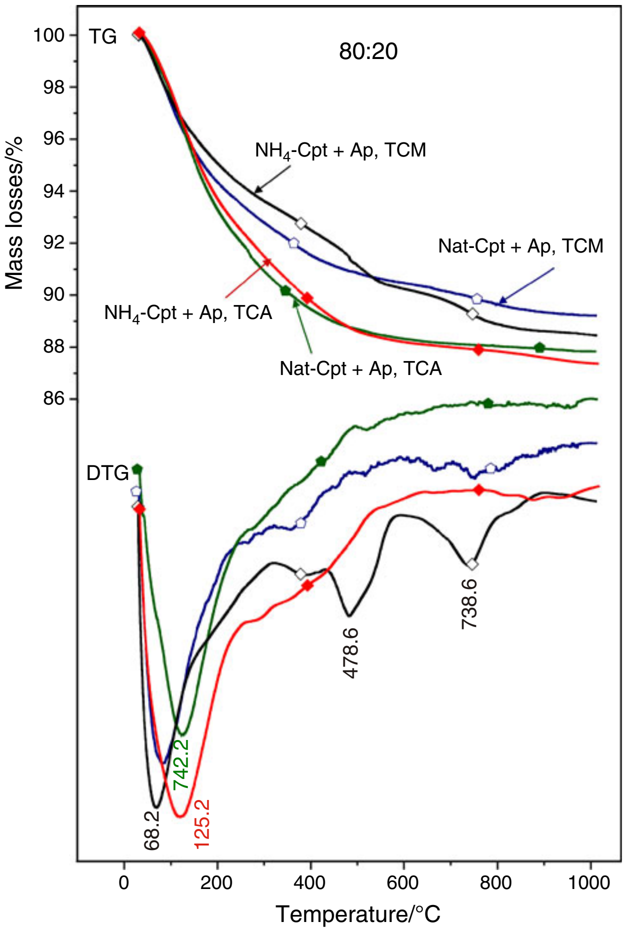

Fig. 6 TG–DTG curves of decomposition of of Nat-Cpt/Ap and NH$_4$-Cpt/Ap in mass ratio 80:20

(Figs. 4, 5, and 6; Tables 3 and 4) proceeds following the stages of decomposition of separate components considering their presence in the mixture. Therefore, in mixtures in which Ap is in surplus to Nat-Cpt and NH$_4$-Cpt, the course of the TG–DTA–DTG dependencies is similar to that of pure apatite. Stages of dehydration of zeolitic water and decarbonization of carbonate ions from both the apatite structure and calcite–dolomite structure are clearly expressed (Fig. 4). In the mixture with domination of Nat-Cpt and NH$_4$-Cpt, recorded changes in the course of the curves are similar to the behavior of pure Nat-Cpt and NH$_4$-Cpt where one stage of dehydration and two stages of deamonization are clearly separated.

Phase analysis of solid run-products heated up to 1000 °C reveals the presence of opal-cristobalite, SiO_2, $Ca_4O(PO_4)_2$, and $Ca_5F(PO_4)_3$ (Table 5). The presence of tetracalcium phosphate is probably due to the solid phase synthesis provoked by "in situ" oxygen obtained during the zeolite framework destruction and the mentioned rupture of F–OH–F bonds in apatite structure at this temperature.

Thermal behavior of Tunisian apatite, clinoptilolite, NH$_4$-clinoptilolite, and their mixtures upon TCA

Clinoptilolite In triboactivated samples of Nat-Cpt and NH$_4$-Cpt both stages of dehydration and deamonization retain their nature but an acceleration of processes are observed. The TCA leads to accumulation of structural defects in combination with a highly developed reaction surface. This is the reason for shifting of the thermal effects to lower temperatures (Figs. 2, 3; Tables 3, 4). A significant difference in decomposition of the activated forms of Nat-Cpt and NH$_4$-Cpt is established in stages of dehydration of zeolitic water in the temperature range up to 100 °C. This is a single-staged process for nonactivated samples, while in the case of activated samples it is double-staged. The mass loss in this temperature range also increases as a result of absorbing moisture from the air on the surface of the activated samples. These facts can be explained with the influence of TCA on the zeolite structure and its defects. Probably channel structure undergoes changes and dislocations, and reorientation or rupture of

Table 3 Thermal effects associated with changes in the structure of Nat-Cpt and NH$_4$-Cpt

No.	Sample	I peak 40–150/°C	ΔG/%	II peak 150–250/°C	ΔG/%	III peak 250–450/°C	ΔG/%	IV peak 450–550/°C	ΔG/%
1.	Nat-Cpt	69.9	6	198.3	2.3	324.2	3.8	–	–
2.	Nat-Cpt, TCA	46.4	2.6	–	–	285.1	3.1	–	–
		120.6	7.1						
1.	Nat-Cpt/Ap, 80:20, TCM	85.2	4.6	183	1.3	269.7	1.3	512.7	0.6
						359.2	0.5		
2.	Nat-Cpt/Ap, 80:20, TCA	63.9	1.2	–	–	273.6	1.4	–	–
		125.2	6.4			437.2	2.7		
3.	Nat-Cpt/Ap, 50:50, TCM	62.3	3.5	185.6	0.9	265.4	0.6	–	–
						357.1	1.7		
4.	Nat-Cpt/Ap, 50:50, TCA	55.2	0.9	198.6	1.7	272.2	0.9	–	–
		118.8	4.2			340.7	1.4		
						403.8	1.3		
5.	Nat-Cpt/Ap, 20:80, TCM	85.2	1.2	152	0.5	364	2	535.6	0.4
				220.5	0.4				
6.	Nat-Cpt/Ap, 20:80, TCA	40	0.6	–	–	328.3	1.5	528.8	0.5
		127.5	2.6			437	0.5		
1.	NH$_4$-Cpt	59.9	5.8	223	3.7	–	–	534	3
								568.4 exo	
2.	NH$_4$-Cpt, TCA	51.7	2.1	–	–	365	3	460.9	1.7
		112.5	4.7						
1.	NH$_4$-Cpt/Ap, 80:20, TCM	68.2	3.7	185.5	2.8	380.3	1.3	478.6	1.2
								533.7 exo	0.7
2.	NH$_4$-Cpt/Ap, 80:20, TCA	58	1.4	272.2	1.6	428.9	2.8	–	–
		118.4	6						
3.	NH$_4$-Cpt/Ap, 50:50, TCM	62	2.6	173.8	1.1	366.4	0.7	520.6	0.9
				231.8	0.7	437.2	0.5		
4.	NH$_4$-Cpt/Ap, 50:50, TCA	55.5	1.1	–	–	323.9	3.4	540.2	0.5
		110.5	4.9						
5.	NH$_4$-Cpt/Ap, 20:80, TCM	46.1	1.7	180	0.4	365.6	1.4	476.3	0.3
				234.1	0.4				
6.	NH$_4$-Cpt/Ap, 20:80, TCA	47.6	0.6	178.4	1.9	332.6	1.9	495.5	0.5
		103.9	2.9			422.6	0.4		

the zeolite framework bonds. These changes lead to cleavage of endothermic effects and DTG dependences in the stage of dehydration of the first zeolitic water. The assumption is confirmed by IR spectra of activated samples of Nat-Cpt and NH$_4$-Cpt, presented in Fig. 7 where a new vibration band at 900 cm^{-1} is detected (ν_3, asymmetric stretching mode T–O–T, T = Si, Al). This band misses in nonactivated samples while in activated samples it is related to the process of deformation and rupture of the intertetrahedral bonds—Si–O–Si or Si–O–Al [23]: as a result active centers are formed, which then interact with the phosphate.

The final products of heating of Nat-Cpt and NH$_4$-Cpt are given in Table 5.

Tunisian phosphorite Changes in the thermal behavior of apatite have also been established. Generally, they are connected with the increased mass loss (from 0.8 to 3.9%) in the temperature range up to 200 °C and its reduction (from 5.7 to 5.4%) in the stage of decarbonization (520–840 °C) (Fig. 3; Table 4). In the temperature range 560–840 °C a new endothermic peak is registered at 527 °C. The 5.4% mass loss summarizes the losses, related to the new thermal reaction at 527 °C, the loss of decarbonization of carbonate ions from B-type positions and from free calcite/dolomite, and that one related to the transformation of C-OH-F-Ap into $Ca_4O(PO_4)_2$.

It has been shown, that under similar conditions of triboactivation, nano-sized grades of about 10–20 nm has

Table 4 Thermal effects associated with changes in the Ap during the TCA

No.	Sample	B-type C-Ap		Calcite		C-OH-F-Ap	
		T_{inf}/°C	Mass losses/%	T_{inf}/°C	Mass losses/%	T_{inf}/°C	Mass losses/%
1.	C-Ap	669.4	2.5	761.0	2.1	830.4	1.1
2.	C-Ap, TCA	695.8	2.2	745.5	1.0	786.7	1.2
1.	Nat-Cpt/Ap, 20:80, TCM	711.5	1.4	775.6	1.4	838.3	1.0
2.	Nat-Cpt/Ap, 20:80, TCA	676.0	1.5	717.2	1.2	835.4	1.0
3.	Nat-Cpt/Ap, 50:50, TCM	671.6	0.5	742.2	0.9	811.3	0.5
4.	Nat-Cpt/Ap, 50:50, TCA	650.5			1.5		
5.	Nat-Cpt/Ap, 80:20, TCM	663.2	0.3	746.4	0.5	–	–
6.	Nat-Cpt/Ap, 80:20, TCA	–	–	–	–	–	–
1.	NH_4-Cpt/Ap, 20:80, TCM	659.0	1.0	730.2	1.4	793.7	1.1
2.	NH_4-Cpt/Ap, 20:80, TCA	–	–	713.3	1.1	824.4	1.1
3.	NH_4-Cpt/Ap, 50:50, TCM	663.2	0.6	729.9		2.2	
4.	NH_4-Cpt/Ap, 50:50, TCA			757.2	1.1		
5.	NH_4-Cpt/Ap, 80:20, TCM	–	–	738.6	1.3	828.6	0.3
6.	NH_4-Cpt/Ap, 80:20, TCA	–	–	–	–	–	–

Table 5 XRD data of samples heated up to 1000 °C

Sample	Identified phases
Nat-Cpt	Opal-cristobalite [16], Quarz, K-feldspar and Albite, Al_2SiO_5
Nat-Cpt, TCA	Opal-cristobalite [16], Quarz, K-feldspar and Albite, Al_2SiO_5
NH_4-Cpt	Opal-cristobalite [16], Quarz, Al_2SiO_5
NH_4-Cpt, TCA	Opal-cristobalite [16], Quarz, Al_2SiO_5
Nat-Cpt/Ap, 50:50, TCM	Opal-cristobalite [16], $Ca_5F(PO_4)_3$, SiO_2, $Ca_4O(PO_4)_2$
Nat-Cpt/Ap, 50:50, TCA	Opal-cristobalite [16], $Ca_5F(PO_4)_3$, SiO_2, $Ca_4O(PO_4)_2$, $Ca_2SiO_4.Ca_3(PO_4)_2$
NH_4-Cpt/Ap, 50:50, TCM	Opal-cristobalite [16], $Ca_5F(PO_4)_3$, SiO_2, $Ca_4O(PO_4)_2$
NH_4-Cpt/Ap, 50:50, TCA	Opal-cristobalite [16], $Ca_5F(PO_4)_3$, SiO_2, $Ca_4O(PO_4)_2$, $Ca_2SiO_4 \cdot Ca_3(PO_4)_2$
Tunisian phosphorite	$Ca_5F(PO_4)_3$, CaF_2, β-$Ca_3(PO_4)_2$
Tunisian phosphorite, TCA	$Ca_5F(PO_4)_3$, CaF_2, α-$Ca_2P_2O_7$, $Ca_4O(PO_4)_2$

been obtained [24–26]. The treatment results in decrease of the apatite structure stability and the formation of a nanosized metastable phase with high chemical reactivity. This leads to the defectiveness and isomorphism of natural apatite structure. Both hydroxyl and carbonate ions take part in the isomorphic transformation by partial substitution of the phosphate by carbonate group (B-type (B1 and B2) substitutions), the fluorine ion by carbonate one (A-type (A1 and A2) and AB substitutions), and the fluorine by hydroxyl ion [1, 27–30].

Due to the weak-bonded interaction of the carbonate ions in A-type positions, they are thermally less stable compared with carbonate ions in B-type positions and the carbonate ions in calcite and dolomite [1, 31].

Based on the comprehensive analysis of data from the physical methods used, it is considered that the changes in the temperature range 520–840 °C are related to isomorphic substitutions in the apatite structure. The new endothermic peak at 530 °C is explained by the decomposition of carbonate ions occupying the A-type positions. This process is completed at lower temperature as compared to that one of other type of carbonate ion due to weaker bonding in the structure. The data in Table 4 show that mass losses in this temperature range increase while mass losses related to the decarbonization of carbonate ions in B-type position and carbonate admixtures decrease. A probable explanation of this fact is the migration of carbonate ions from the occupied tetragonal position of phosphorous ions to the channels near the hexagonal axis [32].

More significant is the reduction of losses due to calcite and dolomite decomposition (approximately 1.1%). Probably, calcite as a soft mineral (MSH = 3), partially decomposes during triboactivation. It is very likely, that some of the released carbonate ions are introduced in the structure of apatite in the A-type positions, while some of

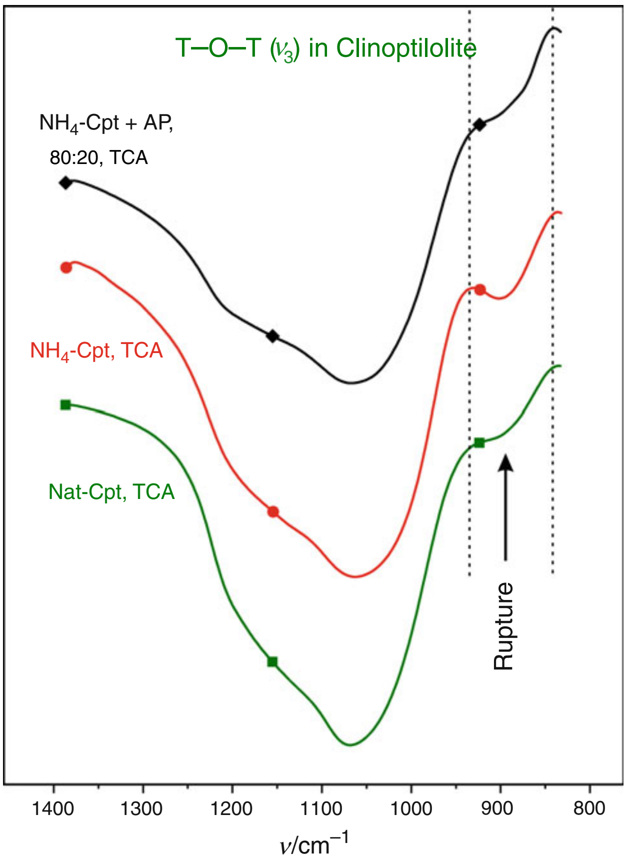

Fig. 7 IR spectra of activated Nat-Cpt and NH$_4$-Cpt and mixture NH$_4$-Cpt + Ap, in the ratio 80:20 in 800–1400 cm^{-1}

them are released as a gas phase. Similar changes are established in the position of the hydroxyl ion.

An increased amount of OH$^-$ in fluorine chains is observed upon TCA: in the temperature interval 760–840 °C the mass losses increase (Table 4). The F–OH–F bonds are ruptured and tetracalcium phosphate is obtained in the solid phase at high temperature (reaction 4).

XRD data indicate the presence of $Ca_5F(PO_4)_3$, CaF_2, α-$Ca_2P_2O_7$, and $Ca_4O(PO_4)_2$ in the solid reminder of decomposition of TCA apatite (Table 5). The formation of pyrophosphate is possible as an additional solid phase reaction at temperature above 700 °C [20, 24].

Mixtures of Nat-Cpt/Ap and NH$_4$-Cpt/Ap A common indication for decomposition in all mixtures is the increase of nearly 4% of the overall mass loss compared with that one for nonactivated mixtures—from 9.0% (a mixture of nonactivated Nat-Cpt/Ap, 20:80) to 13.1% (activated mixture Nat-Cpt/Ap, 50:50). In all active mixtures, the same split endothermic peak of zeolite water (Table 4) is recorded, accompanied with increasing mass loss. In Figs. 4, 5, and 6, the cleavage is not well-expressed, because the activation accelerates the processes of decomposition. Thus, an broad peak is registered in Figs. 4, 5, and 6, which contains two overlapping thermal events. In the triboactivated mixtures Nat-Cpt/Ap and NH$_4$-Cpt/Ap (50:50) and Nat-Cpt/Ap and NH$_4$-Cpt/Ap (80:20) the stages of decomposition of the carbonate-contained components almost completely disappear (see Table 4). In these mixtures, conversion intervals of A into both B-type C-OH-F-Ap and carbonate impurities are removed entirely at the temperatures of decomposition of Cpt. It is believed that the increase of the mass loss is result of the absorbed moisture from the air after triboactivation [20, 31].

X-ray phase analysis of solid decomposition products identified the following phases: opal-cristobalite [16], $Ca_5F(PO_4)_3$, SiO_2, $Ca_4O(PO_4)_2$, $Ca_2SiO_4{\cdot}Ca_3(PO_4)_2$. Calcium phosphate silicate occurs only when the thermal treatment of activated mixtures is applied. It is probably due the presence of octahedral and tetrahedral fragments of Cpt framework structure after its destruction influenced by the formation of active centers on the surface of the mixtures.

The investigations presented here in the system clinoptilolite/apatite demonstrate good prospects for the combined treatment of both components: Clinoptilolite is suitable as an ion-exchanger at soft conditions whereas natural apatite reveals its properties only upon triboactivation due to its chemical and thermal stability.

The preparation of chemically active solid phase as a result of triboactivation gives possibility to apply this method for low-quality apatite raw materials widespread in Bulgaria. An appropriate way to improve the effectiveness of the clinoptilolite/apatite mixture could be obtained by the addition of some technogenic products such as wastes of thermo-electric power stations containing CaO and solid wastes containing N and S. This will be the subject of our future investigations.

Conclusions

1. The highest degree of transformation of non-assimilated into assimilated P_2O_5 was obtained in the NH$_4$-Cpt/Ap mixture with a ratio above 50:50 upon TCM. Nutrient release of the system at these conditions was represented combining dissolution and ion-exchange reaction. The presence of NH$_4^+$ favors the increase of nitrogen in the system and improves the soil fertility.
2. TCA is a suitable method for increasing the reactivity of the chemically inactive natural apatite. This method leads to a high degree of defectiveness and isomorphism in the apatite structure and to accumulation of energy which promotes chemical reaction in the desired directions.

3. The combined use of thermal analysis, powder XRD, and IR spectroscopy provides opportunity to determine the main aspects of the structural and phase transformations and reactions of solid phase synthesis in the investigated systems.

Acknowledgements The authors thank the National Fund ''Scientific research'' of the Ministry of Education for the financial support (project DO O2-104).

References

1. Chaikina MV. Chapter 1: Isomorphous modifications of apatite as the subject of investigations of mechanochemical processes. Chapter 5: Physicochemical transformations and properties of mechanically activated isomorphous modifications of apatite. Chapter 6: Physicochemical transformations of the minerals of phosphate ores under mechanical activations. In: Avvakumov EG, editor. Mechanochemistry of natural and synthetic apatites. Novosibirsk: Publishing house of SB RAS, Branch "GEO"; 2002. p. 11–15, 105–107, 114–115, 139.
2. Wieczorek-Ciurowa Kr, Gamrat K. Mechanochemical syntheses as an example of green processes. J Therm Anal Calorim. 2007;88:213–7.
3. Allen ER, Ming DW. Recent progress in the use of natural zeolites in agronom and horticulture. In: Ming DW, Mumpton FA, editors. Natural Zeolites'93: Occurrence, Properties, Use. International Committee on Natural Zeolites, New York: Brockport; 1993. p. 477–490.
4. Yusupov TS, Shumskaya LG, Kirillova EA, Boldyrev VV. Reactivity of mechanically activated apatite and its interaction with zeolites. J Min Sci. 2006;42(2):189–94.
5. Yusupov TS, Shumskaya LG. Control of cation-exchange interaction between zeolites and phosphates on the basis of soft mechanochemical activation. J Min Sci. 2002;38(2):177–81.
6. Toneva A, Petrova N, Bakardjieva S. Tribochemical reactions between natural phosphates and zeolites. In: Proc. Kontact'97, Sofia; 1997. p. 45–55.
7. Tomazovic Br, Ceranic T, Sijaric G. The properties of NH_4-Clinoptilolite. Part 1. Zeolites. 1996;16:301–8.
8. Petrova N, Filizova L, Kirov G. Callorimetric study of ion-exchange on clinoptilolite and mordenite at different temperatures. In: Kirov G, Filizova L, Petrov O, editors. Natural zeolites—Sofia'95. Sofia, Moscow: Pensoft Publisehrs; 1997. p. 173–81.
9. Petkova V, Kalvachev Yu, Yaneva V. Phase transformations of mechanically activated nano-sized tunisian natural apatite. In: Balabanova E, Dragieva I, editors. Proceedings of X Workshop "Nanoscience & Nanotechnology", 27–28 Nov 2008, ISSN 1313-8995, Sofia: Heron Press; 2009. p. 239–243.
10. Veiderma M, Knubovets R, Tonsuaadu K. Fluorhyroxyapatites of Northen Europe and their thermal transformations, Phosphorus. Sulphur Silicon. 1996;109–110:43–7.
11. Penel G, Leroy G, Rey C, Sombret B, Huvenne JP, Bres E. Infrared and Raman microspectrometry study of fluor-fluor-hydroxyl and hydroxyl-apatite powders. J Mater Sci: Mater Med. 1997;8:271–6.
12. Lai T-M, Elerl D. Controlled and renewable release of phosphorous in soils from mixtures of phosphorous in soils from mixtures of phosphate rock and NH_4-exchanged clinoptilolite. Zeolites. 1986;6:129–32.
13. Yörükoğulları E, Yılmaz G, Dikmen S. Thermal treatment of zeolitic tuff. J Therm Anal Calorim. 2010;100:925–8.
14. Erdoğan BA, Sakizci M, Yörükoğullari E. Investigation of clinoptilolite rich natural zeolites from Turkey: a combined XRF, TG/DTG, DTA and DSC study. Therm Anal Calorim. 2010;100:19–26.
15. Tomazovic Br, Ceranic T, Sijaric G. The properties of NH_4-clinoptilolite. Part 2. Zeolites. 1996;16:309–12.
16. Ilieva A, Mhailova B, Tsintsov Z, Petrov O. Structural state of microcrystalline opals: a Raman spectroscopic study. Am Mineral. 2007;92(8–9):1325–33.
17. Tonsuaadu K, Peld M, Leskela T, Mannonen R, Niinisto L, Veiderma M. A thermoanalytical study of synthetic carbonate-containing apatites. Thermochim Acta. 1995;256:55–65.
18. Lafon JP, Champion E, Bernache-Assollant D, Gibert R, Danna AM. Thermal decomposition of carbonated calcium phosphate apatites. J Therm Anal Calorim. 2003;72:1127–34.
19. Ivanova TI, Frank-Kamenetskaya OV, Kol'tsov AB, Ugolkov VL. Crystal structure of calcium-deficient carbonated hydroxyapatite. Thermal decomposition. J Solid State Chem. 2001;160:340–9.
20. Petkova V, Yaneva V. Thermal behavior and phase transformations of nanosized apatite (Syria). J Therm Anal Calorim. 2010;99(1):179–89.
21. Petkova V, Yaneva V. Thermal investigations on phase transformations of Syrian phosphorite: Part I. J Therm Anal Calorim. 2010;100(1):51–6.
22. Senamaud N, Bernach-Assollant D, Champion E, Heughebaert M, Rey C. Calcination and sintering of hydroxyfluorapatite powders. Solid State Ionics. 1997;101–103:1357–62.
23. Shumskaya LG, Kirillova EA, Yusupov TS. Controlled changes in technological properties of phosphates in mechanical activation with zeolites. J Min Sci. 1999;35(1):96–100.
24. Petkova V, Yaneva V, Pelovski Y. Phase transformation of mechanically activated nano-sized Tunisian carbonate substituted Apatite. Part I. J Balkan Tribol Assoc. 2009;15(4):480–92.
25. Petkova V, Kalvachev Yu, Petrov O. Investigation of structural and spectroscopic properties of nano-sized natural apatites. In: Rositsa Petrova Nikolova, Petrov O, Kovacheva D, Kostov-Kytin V, Shivachev B, Tzvetanova Ya, editors. Ist National Crystallographic Symposium, ISSN 1313-9991, Sofia; 2009. p. 74–77. http://www.clmc.bas.bg/symp09/docs/First_Cryst_Symp.pdf.
26. Yaneva V, Petrov O, Petkova V. Structural and spectroscopic studies of the nanosize appatite (Syrian). Mater Res Bull. 2009;44:693–9.
27. Fleet ME. Infrared spectra of carbonate apatites: ν_2-region bands. Biomaterials. 2009;30:1473–81.
28. Fleet ME, Liu X. Carbonate apatite type A synthesized at high pressure: new space group (P3) and orientation of channel carbonate ion. J Solid State Chem. 2003;174:412–7.
29. Fleet ME, Liu X, King PL. Accommodation of the carbonate ion in apatite: an FTIR and X-ray structure study of crystals synthesized at 2–4 GPa. Am Mineral. 2004;89:1422–32.
30. Fleet ME, Liu X. Accommodation of the carbonate ion in fluorapatite synthesized at high pressure. Am Mineral. 2008;93:1460–9.
31. Chaikina MV, Kryukova GN. Structural transformations in quartz and apatite on mechanical activation. J Struct Chem. 2004;45:S121–6.
32. Lafon JP, Championa E, Bernache-Assollant D. Processing of AB-type carbonated hydroxyapatite $Ca_{10-x}(PO_4)_{6-x}(CO_3)_x(OH)_{2-x-2y}(CO_3)_y$ ceramics with controlled composition. J Eur Ceram Soc. 2008;28:139–47.